

Density Functional Study on Activation and Ion-Pair Formation in Group IV Metallocene and Related Olefin Polymerization Catalysts

Mary S. W. Chan, Kumar Vanka, Cory C. Pye, and Tom Ziegler*

Department of Chemistry, University of Calgary, Calgary, Alberta, Canada T2N 1N4

Received May 4, 1999

The enthalpy of activation by $B(C_6F_5)_3$ and subsequent ion pair formation for the mono(cyclopentadienyl), constrained-geometry, and bis(cyclopentadienyl) titanium and zirconium precatalysts were investigated by DFT methods. Solvation effects were incorporated by single-point calculations using the conductor-like screening model, and where appropriate, a single molecule of the solvent was included to model the short-range solvent–solute interactions. The enthalpy of methide abstraction to form a contact ion pair was exothermic for all systems investigated, and the electron-donating ability of the ligands around the metal center has the most predominant effect on its magnitude. Subsequent studies focused on the reactions of this contact ion pair with the olefin and the solvent (toluene). The insertion of ethylene between the cationic and the anionic moieties was found to be an endothermic process for all six catalyst precursors investigated. The bis(cyclopentadienyl) systems showed the least endothermic ethylene complexation energy of 6.1 and 8.2 kcal/mol for the titanium and zirconium precatalysts, respectively. The insertion of toluene between the contact ion pair was found to be exothermic for both the mono(cyclopentadienyl) and the zirconium constrained-geometry catalysts but endothermic for the titanium constrained-geometry catalyst and both of the bis(cyclopentadienyl) catalysts. The bulky ligands hinder the approach of the toluene in the bis(cyclopentadienyl) systems, making olefin complexation the more competitive route. The strong tendency for the mono(cyclopentadienyl) and constrained-geometry systems to coordinate with toluene may be an obstacle to olefin complexation.

I. Introduction

Single-site homogeneous catalysts have been receiving increasing attention over traditional Ziegler–Natta type heterogeneous catalysts. This is primarily due to their superior performance in achieving higher stereoselectivity, narrower molecular weight distribution, and higher activity. Another advantage is that these systems produce structurally well-defined mononuclear active species. Systematic modification of these structures allows for enhanced control over polymer properties. Among the more highly active homogeneous catalysts are metallocenes and related organometallic compounds containing a group 4 transition metal. The metallocenes by themselves are not very effective as polymerization catalysts but require activation by a cocatalyst. The general structures of these precatalysts contain a transition-metal center coordinated to two ligands (L) and two alkyl groups. The cocatalysts are generally Lewis acids whose function is to abstract one of the alkyl groups to produce the activated metal catalyst, which is generally accepted to be an electrophilic species with cationic character.

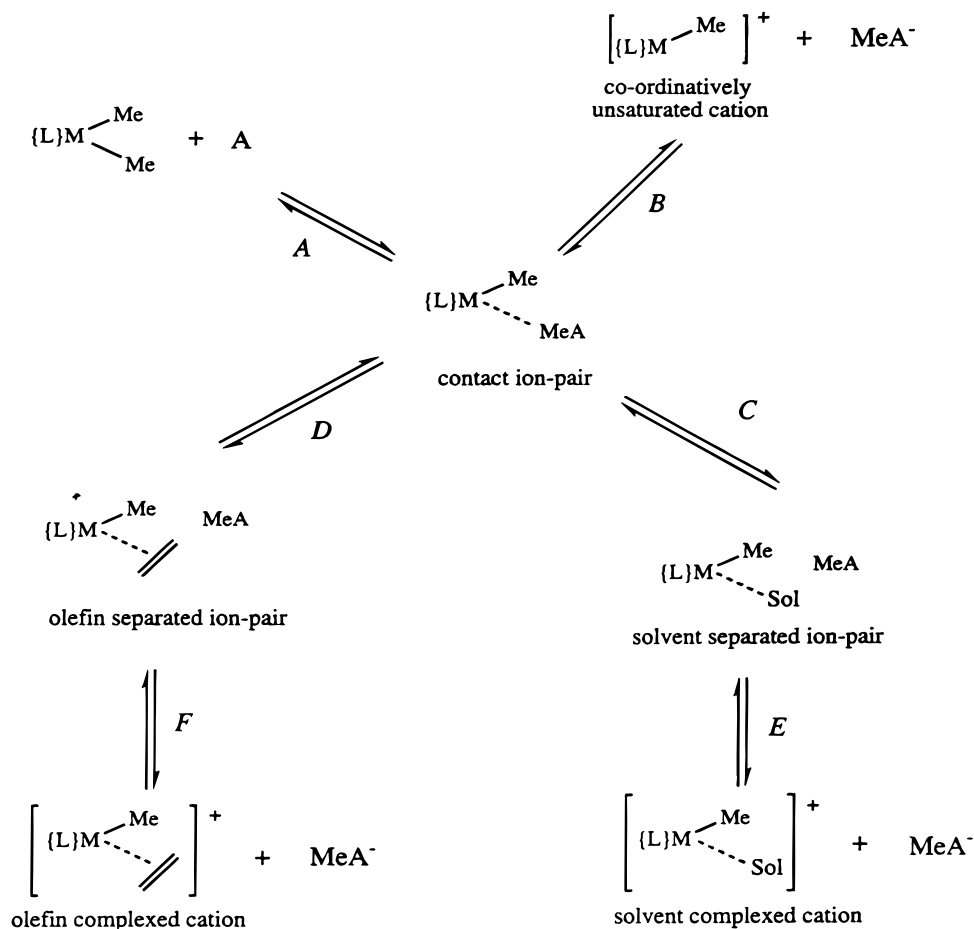
The activation of the dialkyl precatalysts using a variety of cocatalysts such as boranes,¹ carboranes,² and aluminum-based³ systems has been investigated experimentally. There is strong experimental evidence to suggest that the cocatalyst and solvent have strong effects on catalyst activity.⁴ The isolated products as well as in situ NMR studies indicate the formation of a variety of species associated with the metallocene catalyst, the cocatalyst, the solvent, and the olefin. A complex equilibrium is established between these species when the polymerization is carried out in solution. A possible schematic of this equilibration is depicted in Scheme 1. The activation of the dimethyl precatalyst by a Lewis acid can lead to the formation of a contact ion pair in which the cocatalyst is coordinated to the

(1) (a) Jia, L.; Yang, X.; Ishihara, A.; Marks, T. J. *Organometallics* **1995**, *14*, 3135. (b) Deck, P. A.; Marks, T. J. *J. Am. Chem. Soc.* **1995**, *117*, 6128. (c) Jia, L.; Yang, X.; Stern, C. L.; Marks, T. J. *Organometallics* **1997**, *16*, 842. (d) Wang, Q.; Quyoum, R.; Gillis, D. J.; Jeremic, D.; Tudoret, M.-J.; Baird, M. C. *J. Organomet. Chem.* **1997**, *527*, 7. (e) Yang, X.; Stern, C. L.; Marks, T. J. *J. Am. Chem. Soc.* **1994**, *116*, 10015. (f) Chen, Y.-X.; Marks, T. J. *Organometallics* **1997**, *16*, 3649.

(2) (a) Hlatky, G. G.; Turner, H. W.; Eckman, R. R. *J. Am. Chem. Soc.* **1989**, *111*, 2728. (b) Hlatky, G. G.; Eckman, R. R.; Turner, H. W. *Organometallics* **1992**, *11*, 1413. (c) Crowther, D. J.; Borkowsky, S. L.; Swenson, D.; Meyer, T. Y.; Jordan, R. F. *Organometallics* **1993**, *12*, 2897.

(3) (a) Siedle, A. R.; Newmark, R. A.; Lamanna, W. M.; Schroeffer, J. N. *Polyhedron* **1990**, *9*, 301. (b) Bochmann, M.; Lancaster, S. J. *Angew. Chem., Int. Ed. Engl.* **1994**, *33*, 1634. (c) Bochmann, M.; Lancaster, S. J. *J. Organomet. Chem.* **1995**, *497*, 55.

(4) (a) Chen, Y.-X.; Stern, C. L.; Marks, T. J. *J. Am. Chem. Soc.* **1997**, *119*, 2582. (b) Jia, L.; Yang, X.; Stern, C. L.; Marks, T. J. *Organometallics* **1997**, *16*, 842. (c) Chen, Y.-X.; Stern, C. L.; Marks, T. J. *J. Am. Chem. Soc.* **1996**, *118*, 12451. (d) Giardello, M. A.; Disen, M. S.; Stern, C. L.; Marks, T. J. *J. Am. Chem. Soc.* **1995**, *117*, 12114. (e) Tritto, I.; Donetti, R.; Sacchi, M. C.; Locatelli, P.; Zannoni, G. *Macromolecules* **1999**, *32*, 264. (f) Tritto, I.; Donetti, R.; Sacchi, M. C.; Locatelli, P.; Zannoni, G. *Macromolecules* **1997**, *30*, 1247.

Scheme 1. Possible Reactions of the Contact Ion Pair under Typical Polymerization Conditions

metal center as shown in pathway A of Scheme 1. In some cases, the cocatalyst becomes negatively charged after methide abstraction and, therefore, also plays the role of the counterion. Once produced in the reaction mixture, the contact ion pair can dissociate into completely solvated cation and anion as in path B. Alternatively, a molecule of the solvent can interact with the cationic moiety, pushing away the anion to form the solvent-separated ion pair as shown in pathway C of Scheme 1. Pathway E indicates that further solvation of such an ion pair can lead to the formation of a solvent complexed cation with the counterion sufficiently far away that no electrostatic interaction is possible. In the presence of the olefin, a molecule of the olefin can insert itself between the contact ion pair in a similar fashion to produce the olefin separated ion pair (pathway D). Further dissociation of this ion pair results in the formation of the olefin-complexed cation as shown in pathway F of Scheme 1.

Another advantage of the well-defined molecular structure of these metallocene catalysts is that they

allow for more thorough mechanistic studies by theoretical methods. Many theoretical studies have been conducted on the olefin uptake, insertion, and termination steps of the polymerization process,⁵ but comparatively little has been reported on the first step: the activation.⁶ Lanza et al.^{6a} studied the activation of the titanium constrained-geometry precatalyst by tris(pentafluorophenyl)borane, B(C₆F₅)₃, using ab initio methods. Their calculated enthalpy change for the ion pair formation and dissociation steps differ by 10 kcal/mol from observed experimental values.⁷ However, their results did signify that counterion and solvation effects are substantial in catalyst activation and olefin insertion processes. As demonstrated by Scheme 1, many different pathways can be hypothesized, but relatively little is known about their influence on the polymerization process. It is the aim of this study to fill in the gap by investigating the energetics of these equilibria and discuss their implications on catalyst activity. The study will be focused on the activation of three classes of metallocene-based precatalysts by B(C₆F₅)₃ using density functional methods. The general structures of the precatalysts are shown in Figure 1: the mono(cyclo-

(5) (a) Woo, T. K.; Margl, P. M.; Ziegler, T.; Blöchl, P. E. *Organometallics* **1997**, *16*, 3454. (b) Woo, T. K.; Margl, P. M.; Lohrenz, J. C. W.; Blöchl, P. E.; Ziegler, T. *J. Am. Chem. Soc.* **1996**, *118*, 13021. (c) Margl, P. M.; Lohrenz, J. C. W.; Ziegler, T.; Blöchl, P. E. *J. Am. Chem. Soc.* **1996**, *118*, 4434. (d) Fan, L.; Harrison, D.; Woo, T. K.; Ziegler, T. *Organometallics* **1995**, *14*, 2018. (e) Meier, R. J.; Doremaele, G. H. J. V.; Tarlori, S.; Buda, F. *J. Am. Chem. Soc.* **1994**, *116*, 7274. (f) Yoshida, T.; Koga, N.; Morokuma, K. *Organometallics* **1995**, *14*, 746. (g) Weiss, H.; Ehrig, M.; Ahlrichs, R. *J. Am. Chem. Soc.* **1994**, *116*, 4919. (h) Bierwagen, E. P.; Bercaw, J. E.; Goddard, W. A., III. *J. Am. Chem. Soc.* **1994**, *116*, 1481.

(6) (a) Lanza, G.; Fragalà, I. L.; Marks, T. J. *J. Am. Chem. Soc.* **1998**, *120*, 8257. (b) Fusco, R.; Lango, L.; Masi, F.; Garbassi, F. *Macromolecules* **1997**, *30*, 7673. (c) Fusco, R.; Lango, L.; Masi, F.; Garbassi, F. *Macromol. Rapid Commun.* **1997**, *18*, 433. (d) Fusco, R.; Lango, L.; Proto, A.; Masi, F.; Garbassi, F. *Macromol. Rapid Commun.* **1998**, *19*, 257.

(7) Deck, P. A.; Beswick, C. L.; Marks, T. J. *J. Am. Chem. Soc.* **1998**, *120*, 1772.

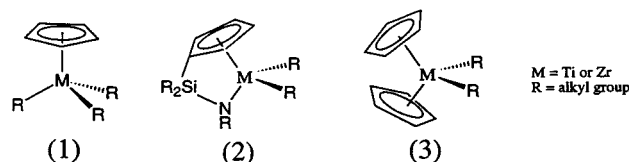


Figure 1. General structures for the mono(cyclopentadienyl), constrained-geometry and bis(cyclopentadienyl) catalyst precursors.

Table 1. Slater Type Basis Functions and Solvation Radii for All Atom Types

atom type	frozen core	valence	polarization	radius, Å
H (Cp)		1s d ζ		1.16
H		1s d ζ	2p s ζ	1.16
B	[He]	2s, 2p d ζ	3d s ζ	1.15
C (Cp)	[He]	2s, 2p d ζ		2.00
C	[He]	2s, 2p d ζ	3d s ζ	2.00
N	[He]	2s, 2p d ζ	3d s ζ	1.40
F	[He]	2s, 2p d ζ	3d s ζ	1.15
Si	[Ne]	3s, 3p d ζ	3d s ζ	2.20
Ti	[Ne]	3s, 3p d ζ ; 3d, 4s t ζ	4p s ζ	2.30
Zr	[Ar]3d ¹⁰	4s d ζ ; 4p, 4d, 5s, t ζ	5p s ζ	2.40

pentadienyl) system (1), the constrained-geometry system (2), and the bis(cyclopentadienyl) system (3).

II. Computational Details

The density functional theory calculations were carried out using the Amsterdam Density Functional (ADF) program (version 2.3.3) developed by Baerends et al.⁸ and vectorized by Ravenek.⁹ The numerical integration scheme applied was developed by te Velde et al.,¹⁰ and the geometry optimization procedure was based on the method of Versluis and Ziegler.¹¹ Geometry optimizations were carried out using the local exchange-correlation potential of Vosko et al.¹² without any symmetry constraints, unless specifically indicated. A triple- ζ or double- ζ basis set was used to describe the valence orbitals, whereas the core orbitals were treated with a frozen-core approximation. Detailed basis sets for the individual atom types used in this study can be found in Table 1.

A set of auxiliary s, p, d, f, and g STO functions centered on all nuclei was used to fit the molecular density and represents Coulomb and exchange potentials accurately in each SCF cycle.¹³ The gas-phase energy difference was calculated by augmenting the local density approximation energy with Perdew and Wang's nonlocal correlation and exchange corrections.¹⁴ The energy difference in solution was corrected from the gas-phase energy by accounting for the solvation energy calculated by the conductor-like screening model (COSMO) that had recently been implemented into the ADF program.¹⁵ The solvation calculations were performed with a dielectric constant of 2.38 to represent toluene as the solvent. The radii used for the construction of the solvent-accessible surface for each atom type are collected in Table 1. These values were obtained by optimization using least-squares fitting to experimental solvation energies. The charge distribution study was

carried out by Hirshfeld analysis.¹⁶ For reference to the various species identified, the three catalyst systems will be identified by Arabic numbers. The letters a–h will, wherever appropriate, indicate compounds for the μ -Me contact ion pair, olefin-separated ion pair, olefin π -complex, coordinately unsaturated cation, μ -F contact ion pair, solvated contact ion pair, solvent-separated ion pair, and solvent-complexed cation, respectively. The metals are denoted by –Ti and –Zr, respectively.

III. Results and Discussion

a. Catalyst Activation. The activation of the dimethyl precursors $\{L\}MMe_2$ by $B(C_6F_5)_3$ for the three classes of catalysts of interest in this study has been examined experimentally.^{1d–f} These studies suggest the formation of the contact ion pair $\{[L]MMe\}^+[MeB(C_6F_5)_3]^-$ as opposed to completely separated ions $\{[L]MMe\}^+$ and $[MeB(C_6F_5)_3]^-$. The ion pairs generated from the (1,2- $Me_2C_5H_3$)ZrMe₂ and (Me_5C_5)₂ZrMe₂ precursors have been characterized by X-ray diffraction studies, while those generated from (Me_5C_5)TiMe₃ and $Me_2Si(Me_4C_5)TiMe_2$ have only been characterized by solution NMR data. The crystal structures of the substituted zirconocenes show that the cationic metal center is bound to the anion via an unsymmetrical Zr–Me–B bridge (Figure 2). The Zr–Me (bridging) bond is on average 0.3 Å longer than the terminal Zr–Me bond, while the B–Me (bridging) bond is just slightly longer than in the free anion $MeB(C_6F_5)_3^-$. The geometries of these crystal structures were used as models for the starting structure in the optimization procedure for the ion pairs in this study. The calculated structures obtained are similar to those of the crystal structures. The optimized structure of the pentamethylzirconocene ion pair is shown in Figure 2, and selected bond distances and angles are collected in Table 2 for comparison with the crystal structure data.

The calculated enthalpy for the methide abstraction reaction is reported in Table 3. These values were obtained by evaluating the energy differences between the neutral precursors and the contact ion pair. As expected, correcting for solvation effects implicitly with the COSMO model does not change the ΔH value significantly, as there is no net charge separation on both sides of the equation. Out of the systems examined in Table 3, the only experimental value reported is for the Cp_2ZrMe_2 precatalyst, where a ΔH value of –23.1 kcal/mol was measured by titration calorimetry.⁷ The calculated value of –19.1 kcal/mol is in reasonable agreement with this number. Another observation that can be made from Table 3 is that changing the metal center also does not cause significant changes in the abstraction energies. Abstraction from titanium precatalysts is 2–3 kcal/mol less favorable than that from the zirconium precatalysts within the same ligand system. This is in reasonably good agreement with the difference of 1.3 kcal/mol obtained from experimental values for $Me_2Si(Me_4Cp)(t-BuN)TiMe_2$ at –22.6 kcal/mol and $Me_2Si(Me_4Cp)(t-BuN)ZrMe_2$ at –23.9 kcal/mol.

Varying the ligands around the metal has a more pronounced effect on the abstraction enthalpy. The mono(cyclopentadienyl) systems have the least negative abstraction energy, followed by the constrained-geom-

- (8) (a) Baerends, E. J.; Ellis, D. E.; Ros, P. *Chem. Phys.* **1973**, *2*, 41. (b) Baerends, E. J.; Ros, P. *Chem. Phys.* **1973**, *2*, 52.
 (9) Ravenek, W. In *Algorithms and Applications on Vector and Parallel Computers*; te Riele, H. J. J., Dekker, T. J., van de Horst, H. A., Eds.; Elsevier: Amsterdam, The Netherlands, 1987.
 (10) (a) te Velde, G.; Baerends, E. J. *J. Comput. Chem.* **1992**, *99*, 84. (b) Boerrigter, P. M.; te Velde, G.; Baerends, E. J. *Int. J. Quantum Chem.* **1988**, *33*, 87.
 (11) Versluis, L.; Ziegler, T. *J. Chem. Phys.* **1988**, *88*, 322.
 (12) Vosko, S. H.; Wilk, L.; Nusair, M. *Can. J. Phys.* **1980**, *58*, 1200.
 (13) Krijn, J.; Baerends, E. J. *Fit Functions in the HFS-Method*; Free University of Amsterdam: Amsterdam, 1984.
 (14) Perdew, J. P. *Phys. Rev. B* **1992**, *46*, 6671.
 (15) Pye, C. C.; Ziegler, T. *Theor. Chim. Acta* **1999**, *101*, 396.

- (16) (a) Hirshfeld, F. L. *Theor. Chim. Acta* **1977**, *44*, 129. (b) Wiberg, K. B.; Rablen, P. R. *J. Comput. Chem.* **1993**, *1412*, 1504.

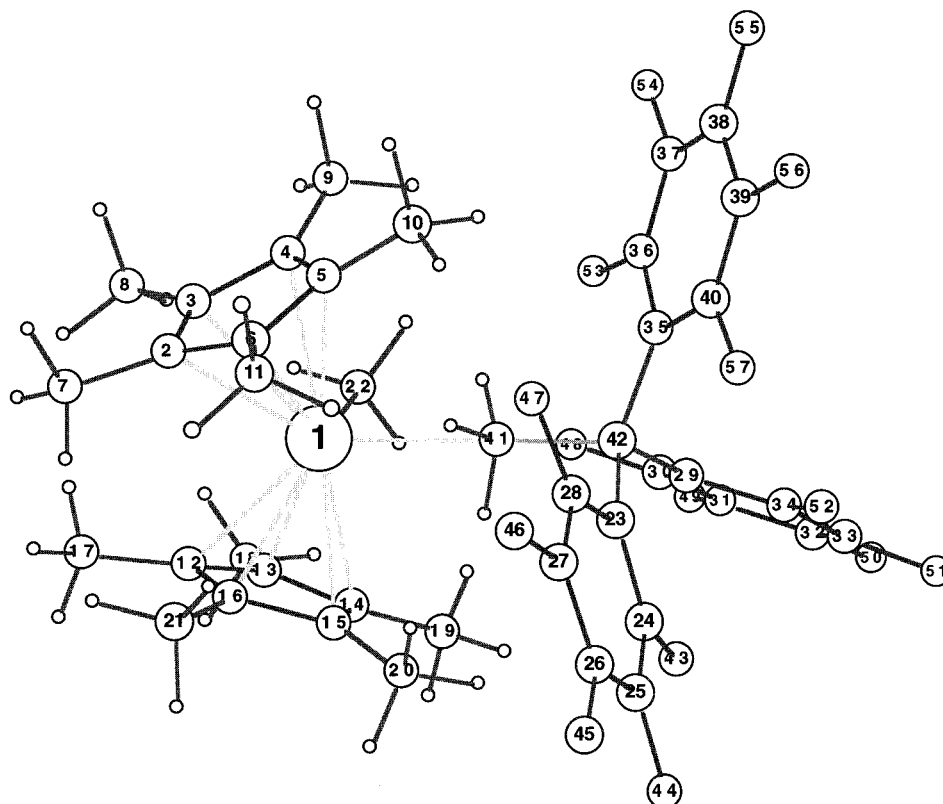


Figure 2. LDA-optimized structure of the $[(\text{Me}_5\text{C}_5)_2\text{ZrMe}]^+[\text{MeB}(\text{C}_6\text{F}_5)_3]^-$ contact ion pair.

Table 2. Selected Bond Distances and Bond Angles for the Crystal Structure and Optimized Structure of $[(\text{Me}_5\text{C}_5)_2\text{ZrMe}]^+[\text{MeB}(\text{C}_6\text{F}_5)_3]^-$

bond distance (Å)			angle (deg)		
	cryst struct ^a	optimized struct		cryst struct ^a	optimized struct
Zr–C ₂	2.558(7)	2.5193	C ₂₃ –B–C ₂₉	111.5(5)	111.32
Zr–C ₃	2.540(7)	2.5136	C ₂₃ –B–C ₃₅	114.6(5)	114.42
Zr–C ₄	2.551(7)	2.5393	C ₂₃ –B–C ₄₁	101.7(5)	101.42
Zr–C ₅	2.534(6)	2.5231	C ₂₉ –B–C ₃₅	104.2(5)	105.15
Zr–C ₆	2.509(6)	2.4814	C ₂₉ –B–C ₄₁	114.3(5)	111.43
Zr–C ₁₂	2.511(7)	2.5138	C ₃₅ –B–C ₄₁	110.9(5)	111.30
Zr–C ₁₃	2.526(7)	2.5209	Zr–C ₄₁ –B	176.6(4)	177.66
Zr–C ₁₄	2.557(7)	2.5312			
Zr–C ₁₅	2.549(7)	2.5164			
Zr–C ₁₆	2.530(7)	2.5029			
Zr–C ₂₂	2.223(6)	2.2546			
B–C ₄₁	1.66(1)	1.6470			
B–C ₂₃	1.666(9)	1.6169			
B–C ₂₉	1.64(1)	1.6144			
B–C ₃₅	1.655(9)	1.6144			

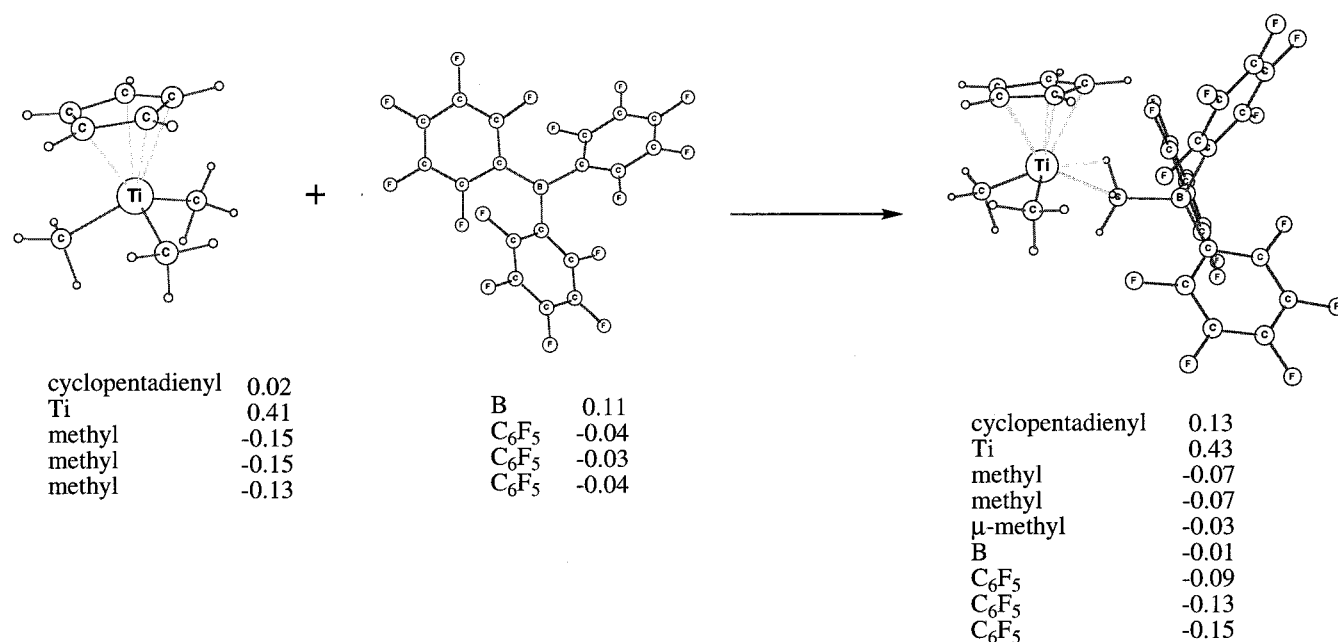
^a Obtained from ref 25.

etry catalysts, and finally the bis(cyclopentadienyl) systems. Ancillary ligands can influence the stability of the contact ion pair relative to the neutral starting materials in two ways: (a) steric repulsion between the ancillary ligands and the anion aryl groups and (b) electronic stabilization of the metal center. The observed trend in ΔH is contrary to expectations when steric effects are considered, as large ancillary ligands should hinder the approach of the bulky Lewis acid $\text{B}(\text{C}_6\text{F}_5)_3$ and thus render the abstraction less favorable. On the other hand, electronic factors are expected to have a strong influence, as the optimized structure of the contact ion pair suggests the formation of a cationic metal fragment and an anionic boron fragment. The charge densities for the neutral precursors and the

Table 3. Enthalpy Change for Methide Abstraction by $\text{B}(\text{C}_6\text{F}_5)_3$: $\{\text{L}\}\text{M}(\text{Me})_2 + \text{B}(\text{C}_6\text{F}_5)_3 \rightarrow [\{\text{L}\}\text{MMe}]^+[\text{MeB}(\text{C}_6\text{F}_5)_3]^-$

catalyst precursor	ΔH (kcal/mol)	
	gas phase	solution
CpTiMe_3	–12.9	–12.2
CpZrMe_3	–15.7	–14.9
$\text{H}_2\text{SiCp}(\text{NH})\text{TiMe}_2$	–13.9	–14.4
$\text{H}_2\text{SiCp}(\text{NH})\text{ZrMe}_2$	–16.6	–17.5
Cp_2TiMe_2	–15.5	–16.3
Cp_2ZrMe_2	–19.1	–19.1

contact ion pair are shown in Figure 3 for the mono-(cyclopentadienyl) titanium system. The charge densities of the individual atoms are summed in such a way as to give the total charge of ligands or the functional groups attached to the metal or the boron. In the neutral catalyst precursor, a positive charge of 0.41 is concentrated on the titanium metal center, with the compensating negative charges provided by the organic ligands. The cyclopentadienyl ring is almost neutral, while the methyl groups contribute about –0.15 each. In the neutral boron Lewis acid, the boron atom carries a positive charge of 0.11 while the compensating negative charge is distributed evenly over the aryl groups. In the ion pair, the positive charge on the titanium remains relatively the same, while the ligands on the titanium now carry significantly less electron density. The boron and the aryl groups all became significantly more negative than in the neutral precursor. The net result is a flow of electron density from the cyclopentadienyl ring and two of the methyl groups into the boron and pentafluorophenyl groups of the ion pair, with the metal fragment gaining a 0.40 positive charge that is compensated by a negative charge of the same magnitude on the boron side.

**Figure 3.** Charge analysis of ligands and functional groups in the neutral precursors and ion pair.**Table 4. Enthalpy Change for Methide Abstraction and Total Charges for the Constrained-Geometry Catalyst Precursor as a Function of Substitution on the Nitrogen Atom:**
 $\text{H}_2\text{SiCp}(\text{NR})\text{TiMe}_2 + \text{B}(\text{C}_6\text{F}_5)_3 \rightarrow [\text{H}_2\text{SiCp}(\text{NR})\text{TiMe}]^+[\text{MeB}(\text{C}_6\text{F}_5)_3]^-$

R	ΔH (kcal/mol)		total charge		
	gas phase	COSMO	neutral	ion pair	change in charge density
H	-13.9	-14.4	-0.21	-0.17	0.04
methyl	-16.1	-16.4	-0.19	-0.13	0.06
isopropyl	-16.9	-17.0	-0.18	-0.12	0.06
<i>tert</i> -butyl	-18.4	-18.0	-0.19	-0.10	0.09

Replacing one methyl group with a nitrogen and a silicon bridge in the mono(cyclopentadienyl) system produces the constrained-geometry catalyst. This results in the ΔH value for methide abstraction being more negative by about 2 kcal/mol. The increase in exothermicity of the abstraction process for the constrained-geometry systems as compared to the mono(cyclopentadienyl) system is due to the fact that the nitrogen atom can serve as a better electron donor than can a methyl group. Replacing a methyl group with a cyclopentadienyl ligand on the mono(cyclopentadienyl) system to form the bis(cyclopentadienyl) system provides an extra stabilization of 4 kcal/mol. This again, can be attributed to the better electron-releasing ability of the cyclopentadienyl ligand.

A more detailed study of the electronic effects of substituents on the ancillary ligands was conducted on the constrained-geometry catalyst and the bis(cyclopentadienyl) catalysts. Table 4 shows the effect of substituting the nitrogen atom in the constrained-geometry catalyst with increasingly large alkyl groups. The enthalpy of methide abstraction slowly but steadily becomes more negative, beginning from the hydrogen-substituted amine to the *tert*-butyl-substituted amine, as indicated by the ΔH values in the second and third columns. Experimental values for this series of catalyst precursors have not been reported. However, a ΔH value

Table 5. Enthalpy for Methide Abstraction as a Function of Substitution on the Cyclopentadienyl Ligand

substitution on Cp	ΔH (kcal/mol)		
	gas phase	COSMO	exptl ^a
H	-19.1	-19.1	-23.1
1,2-dimethyl	-23.8	-24.0	-24.3
pentamethyl	-27.5	-27.8	-36.7

^a Obtained from ref 7.

of -22.6 kcal/mol was measured for the $\text{Me}_2\text{Si}(\text{Me}_4\text{Cp})-(t\text{-BuN})\text{TiMe}_2$ precursor, whose structure is very similar to that of the calculated $\text{H}_2\text{SiCp}(t\text{-BuN})\text{TiMe}_2$ system. Our calculated value of -18.0 kcal/mol is in better agreement with this experimental value than the -13.0 kcal/mol obtained previously from ab initio calculations.⁶ A rough estimate of the electron-donating ability of these substituents can be obtained by looking at the change in charge density that occurs in the transformation from the neutral precursor to the ion pair. The fourth column in Table 4 represents the total charge on the amido ligand in the neutral precursor, while the total charge of the same group in the ion pair appears in the fifth column. In the sixth column is the difference between the previous two columns, and the positive number indicates a loss of electron density from the substituent. The observed trend corresponds to the electron-donating ability of the substituents.

The effect of methyl substitution on the cyclopentadienyl ligand was also investigated for the bis(cyclopentadienyl) system, and the results are summarized in Table 5. Experimental ΔH values for the methide abstraction for this series of precursors are available; the numbers are reproduced in Table 5 for comparison. Although there are differences in the calculated and the experimental values, the observed trends are in agreement, as both found that the abstraction enthalpy becomes more negative with increasing methyl substitution on the Cp rings. This again emphasizes the influence of electronic factors on the exothermicity of

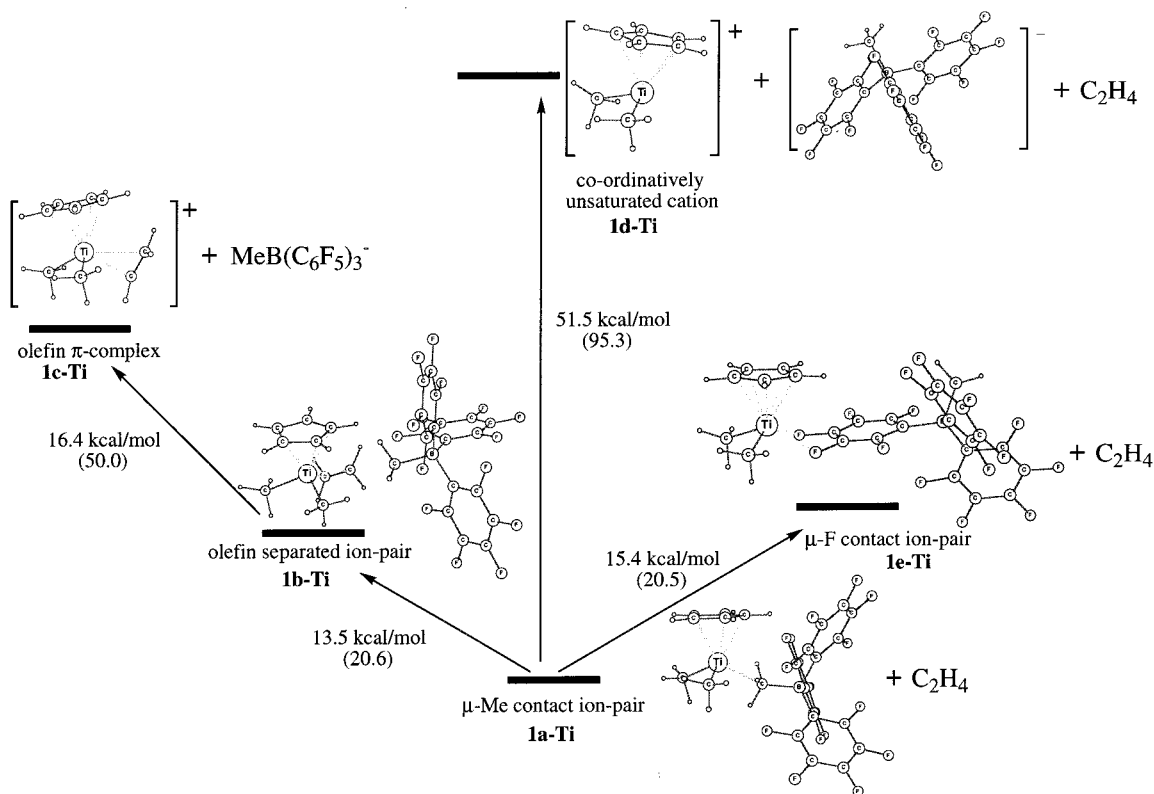


Figure 4. Olefin-complexed ions and ion pairs from the CpTiMe_3 precursor.

methide abstraction. The more substituted pentamethylcyclopentadienyl ligand is a better electron donor, and therefore, it is more effective at stabilizing the developing cationic center on the metal. The higher electron-donating abilities of methyl-substituted cyclopentadienyl ligands have been demonstrated for a variety of different metal centers.¹⁷ The calculated value of -24.0 kcal/mol for 1,2-dimethylzirconocene is in excellent agreement with the experimentally measured value of -24.3 kcal/mol, while the agreement for the unsubstituted zirconocene is poorer, but still reasonable. The major discrepancy between the calculations and the experiments appears in the ΔH value for the pentamethyl analogue. The experimental values show a relatively small change of 1.2 kcal/mol between the unsubstituted and the 1,2-dimethyl-substituted zirconocene with a large gap between the 1,2-dimethyl and the pentamethyl analogues. On the other hand, the calculated values show a more even distribution with respect to methyl substitution. This is in line with previous measurements of ionization and oxidation potential, where a more linear electronic influence was observed with increasing methyl substitution.¹⁷

b. Formation of Separated Ion Pairs. (i) Influence of the Anion on Olefin Complexation. The potential energy surface for the formation of ion pairs for the CpTiMe_3 catalyst precursor is shown in Figure 4. The energies reported include the treatment of solvent effects within the COSMO formalism, while the gas-phase energies are also included in parentheses. The formation of the contact ion pair can occur via a

methyl bridge (1a-Ti), as implied by the crystal structures, but in some cases, metal-fluorine interactions have been detected to suggest a fluorine-bridged ion pair.¹⁸ The structure and energy of the $\mu\text{-F}$ ion pair (1e-Ti) were investigated. In this coordination mode, two of the fluorine atoms on one aryl group are attached to the metal center in a nonsymmetric bridge, similar to those observed for the crystal structure of $(\text{Me}_5\text{Cp})_2\text{ZrH-HB}(\text{C}_6\text{F}_5)_3$.¹⁹ The Ti-F interatomic distances of 2.253 and 2.186 Å are significantly longer than the average terminal Ti-F bond distance of 1.823 Å found in the crystal structure of tetrafluorobis(η^5 -methylcyclopentadienyl)bis(μ -fluoro)(μ -tetrahydrofuran)ditanium.²⁰ There is also a slight elongation of the $\mu\text{-F-C}$ distances to 1.371 and 1.377 Å from the average aryl C-F distance of 1.329 Å. The $\mu\text{-F}$ ion pair (1e-Ti) is much higher in energy (15.4 kcal/mol) than the $\mu\text{-Me}$ ion pair (1a-Ti) for this particular system. This ion pair (e) is of the same order of magnitude above the $\mu\text{-Me}$ contact ion pair (a) for all the other catalyst precursors investigated. Therefore, only the $\mu\text{-Me}$ ion pair (a) is considered in subsequent discussions.

The complexation of the olefin to the metal center must take place in order for the ion pair to initiate polymerization. One possible pathway for the formation of such a species is for the olefin to insert between the cation and the anion of the contact ion pair, binding itself to the vacant coordination site on the metal. The optimized structure for this olefin-separated ion pair (1b-Ti) is shown in Figure 4. The π -bond of the ethylene is oriented parallel to the Cp ring with the two carbon

(17) (a) Gassman, P. G.; Macomber, D. W.; Hershberger, J. W. *Organometallics* **1983**, *2*, 1470. (b) Calabro, D. C.; Hubbard, J. L.; Blevins, C. H., II; Campbell, A. C.; Lichtenberger, D. L. *J. Am. Chem. Soc.* **1981**, *103*, 6839. (c) Miller, E. J.; Landon, S. J.; Brill, T. B. *Organometallics* **1985**, *4*, 533.

(18) Bochmann, M. *J. Chem. Soc., Dalton Trans.* **1996**, 225.

(19) Yang, X.; Stern, C. L.; Marks, T. J. *Angew. Chem., Int. Ed. Engl.* **1992**, *31*, 1375.

(20) Herzog, A.; Liu, F.-Q.; Roesky, H. W.; Demsar, A.; Keller, K.; Noltemeyer, M.; Pauer, F. *Organometallics* **1994**, *13*, 1251.

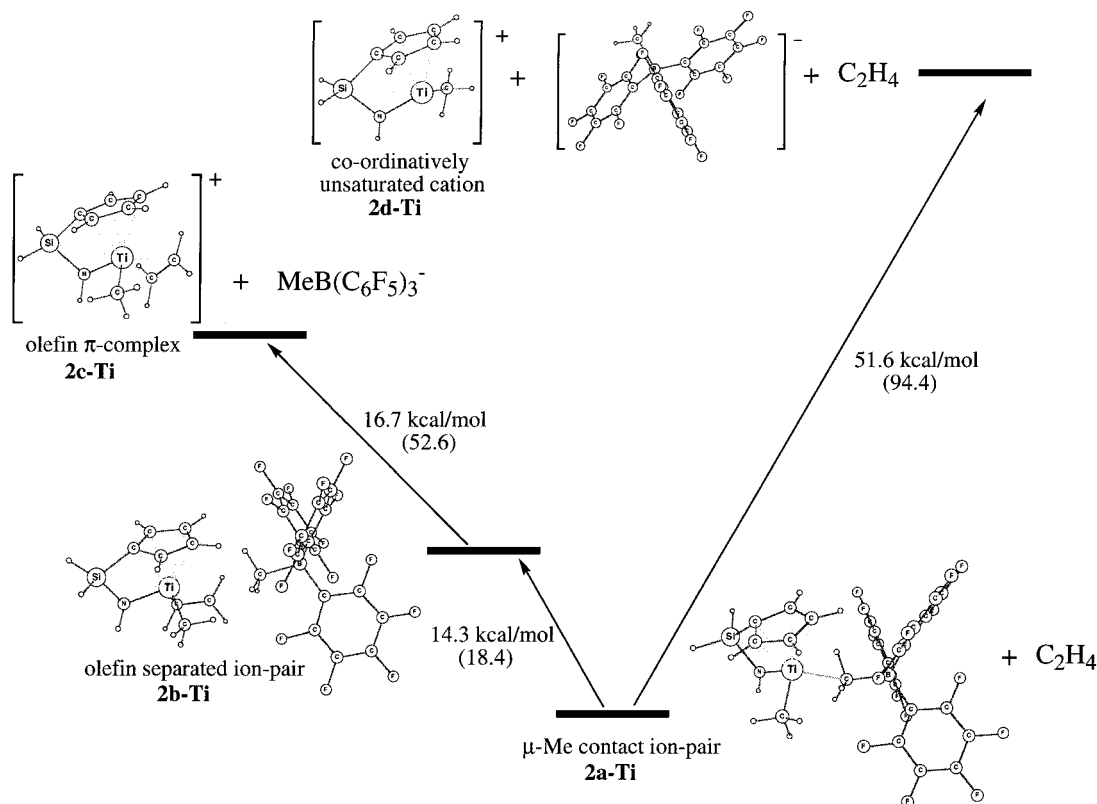


Figure 5. Olefin-complexed ions and ion pairs from the $\text{H}_2\text{SiCp}(\text{NH})\text{TiMe}_2$ precursor.

atoms almost equidistant from the titanium at 2.510 and 2.497 Å. These olefin carbon–titanium distances are just slightly longer than the distances of 2.510 and 2.466 Å found in the optimized structure of the cationic π -complex by itself. The anion, $\text{MeB}(\text{C}_6\text{F}_5)_3^-$, however, has been pushed away from the metal center. The Ti– $\mu\text{-Me}$ distance is now 4.236 Å instead of 2.194 Å in the contact ion pair (**1a-Ti**). For this particular system, the olefin-separated ion pair (**1b-Ti**) is 13.5 kcal/mol higher in energy than the sum of **1a-Ti** and ethylene. Although the structure suggests that the anion is only weakly associated with the π -complex, further dissociation into an olefin-complexed cation (**1c-Ti**) and the anion requires another 16.4 kcal/mol. Surprisingly, the most stable structure found for the isolated ethylene π -complex (**1c-Ti**) does not correspond to the lowest energy structure obtained for the olefin-separated ion pair (**1b-Ti**). The conformer with the ethylene coordinated parallel to the plane of the Cp ring is 2.0 kcal/mol more stable than the one with the ethylene perpendicular to the plane of the Cp ring in the olefin-separated ion pairs. This trend is reversed in the cationic π -complexes, where the conformer with the ethylene perpendicular to the plane of the Cp ring is more stable by 1.0 kcal/mol. Finally, complete dissociation of the contact ion pair (**1a-Ti**) into the “bare” cation CpTiMe_2^+ (**1d-Ti**) and the anion $\text{MeB}(\text{C}_6\text{F}_5)_3^-$ is on the order of 50 kcal/mol. It is worth mentioning that the present study looks at the olefin uptake process from a difference perspective than previous theoretical studies, without considering the anion. In the latter cases, the olefin complexation energy was calculated to be exothermic because the reference energy is the bare cationic catalyst and ethylene.^{5b,d,f} In the present study it is endothermic by 13.5 kcal/mol because the reference was ethylene and the contact ion

pair where the electrophilic metal center is stabilized by the counterion.

The optimized structures for the CpZrMe_3 system are very similar to those obtained for the titanium analogue. The relative energies are also similar, with the exception that, relative to the contact ion pair (**1a-Zr**), the other species on the potential energy surface are located about 2 kcal/mol lower in energy than their corresponding titanium analogues. Another difference is that the olefin-separated ion pair (**1b-Zr**) is only 12.6 kcal/mol higher in energy than the contact ion pair and that dissociation into the completely separated cationic olefin π -complex (**1c-Zr**) and the anion requires a further 18.3 kcal/mol, whereas in the titanium system the energy was 13.5 kcal/mol for the first process and 16.4 kcal/mol for the dissociation, suggesting that the anion is bound more tightly to the zirconium olefin complex than the titanium complex.

The relative energies of the olefin complexes and ion pairs for the constrained-geometry titanium precatalyst $\text{H}_2\text{SiCp}(\text{NH})\text{TiMe}_2$ are shown in Figure 5. The potential energy surface for the zirconium analogue $\text{H}_2\text{SiCp}(\text{NH})\text{-ZrMe}_2$ has similar features and is therefore not reproduced. The behavior of these two systems with regard to olefin complexation is similar to that of the mono-(cyclopentadienyl) systems. The optimized structures are also similar to those of their mono(cyclopentadienyl) counterparts. The contact ion pairs (**2a-Ti** and **2a-Zr**) are connected by an unsymmetric methyl bridge. The M–Me distance is 2.162 Å for titanium and 2.340 Å for zirconium, while the Me–B bond distance is 1.634 Å for both metals. In both structures, two of the hydrogen atoms on the bridging methyl group are sufficiently close to the metal that they provide agostic stabilization. The energies required to form the olefin-separated ion

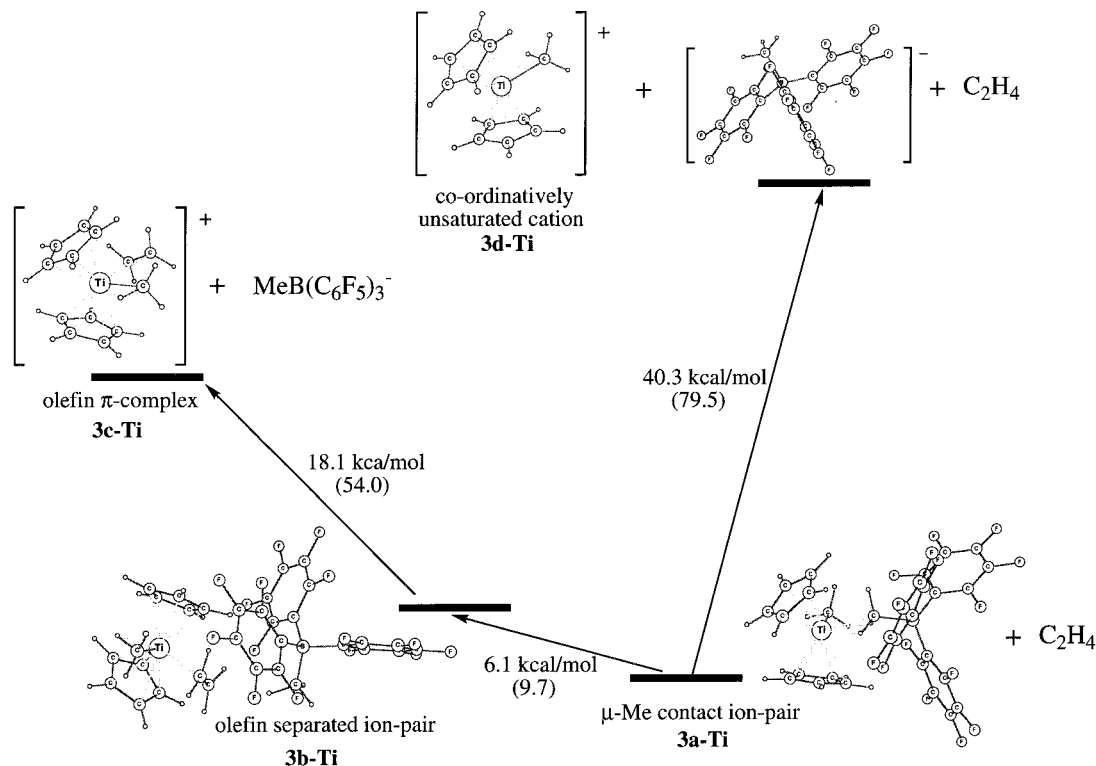


Figure 6. Olefin-complexed ions and ion pairs from the Cp_2TiMe_2 precursor.

pairs (**2b-Ti** and **2b-Zr**) were similar to those for the mono(cyclopentadienyl) systems at 14.3 kcal/mol for titanium and 10.0 kcal/mol for the zirconium catalyst. The complete separation into the olefin-complexed cation and the borate anion from this ion pair requires another 16.7 kcal/mol for the titanium and 20.0 kcal/mol for the zirconium. In contrast to the mono(cyclopentadienyl) systems, the coordination mode where the ethylene lies in a plane parallel to the Cp ring was found to be the more stable conformer in both the olefin-separated ion pairs (**2b-Ti** and **2b-Zr**) and the cationic π -complexes (**2c-Ti** and **2c-Zr**). The complete dissociation into the coordinatively unsaturated cations (**2d-Ti** and **2d-Zr**) with the anions at infinite distance is again the most endothermic of all processes, at roughly 50 kcal/mol in solution.

The relative energies of the ion pairs and separated ions for the Cp_2ZrMe_2 system resemble those of the Cp_2TiMe_2 system; therefore, only the potential energy surface for the titanium precatalyst is shown in Figure 6. The two systems exhibit similar behavior, but there are significant differences in the appearance of the potential energy surface for the formation of ion pairs from their mono(cyclopentadienyl) or constrained-geometry analogues. The first difference is that structures for neither the isolated olefin π -complexes (**3c-Ti** and **3c-Zr**) nor the olefin-separated ion pairs (**3b-Ti** and **3b-Zr**) could be obtained without geometry constraints. Geometry optimizations beginning with initial structures where the ethylene is positioned at 1.5–4.0 Å from the metal all resulted in the polymerization product in which the olefin is already inserted between the M–Me bond. Estimates of the structure and energy for the olefin π -complexes (**3c-Ti** and **3c-Zr**) and the olefin-separated ion pair (**3b-Ti** and **3b-Zr**) were obtained by constraining the distance between the terminal methyl

carbon and one of the ethylene carbons to 2.60 Å. This distance was suggested by a previous study of ethylene insertion into the zirconocene cation to be optimal for the π -complex.²¹ Even with this constraint, the energy required for the formation of the olefin-separated ion pairs (**3b-Ti** and **3b-Zr**) is the smallest found of the three systems investigated: 6.1 kcal/mol for titanium and 8.2 kcal/mol for zirconium. Their structures are slightly different from those obtained for the previous two systems. The geometries of the cationic and anionic portions are similar, but the anion has turned in such a way that one of the aryl groups (instead of the methyl group) points toward the metal center. Further dissociation into the separated cationic olefin complexes (**3c-Ti** and **3c-Zr**) is endothermic by 18.1 kcal/mol for the titanium and 20.4 kcal/mol for the zirconium. The infinitely separated cations (**3d-Ti** and **3d-Zr**) and anions lie 40.3 and 48.5 kcal/mol above the contact ion pairs for titanium and zirconium, respectively. This confirms again that the coordinatively unsaturated cation is most likely nonexistent in solution.

(ii) Influence of the Solvent on Ion-Pair Formation. The influence of the solvent on ion pair formation was modeled by explicitly including one molecule of toluene to be treated quantum mechanically along with the solute. The potential energy surface for the formation of complexes and ion pairs associated with the solvent for the mono(cyclopentadienyl) titanium system appears in Figure 7. One molecule of toluene was added to the outside of the contact ion pair (**1a-Ti**) to determine the short-range solvent–solute interactions. This “solvation” does not cause notable changes in the relative stability compared to the contact ion pair alone. The optimized structure of the solvated contact ion pair

(21) Lohrenz, J. C. W.; Woo, T. K.; Fan, L.; Ziegler, T. *J. Organomet. Chem.* **1995**, 497, 91.

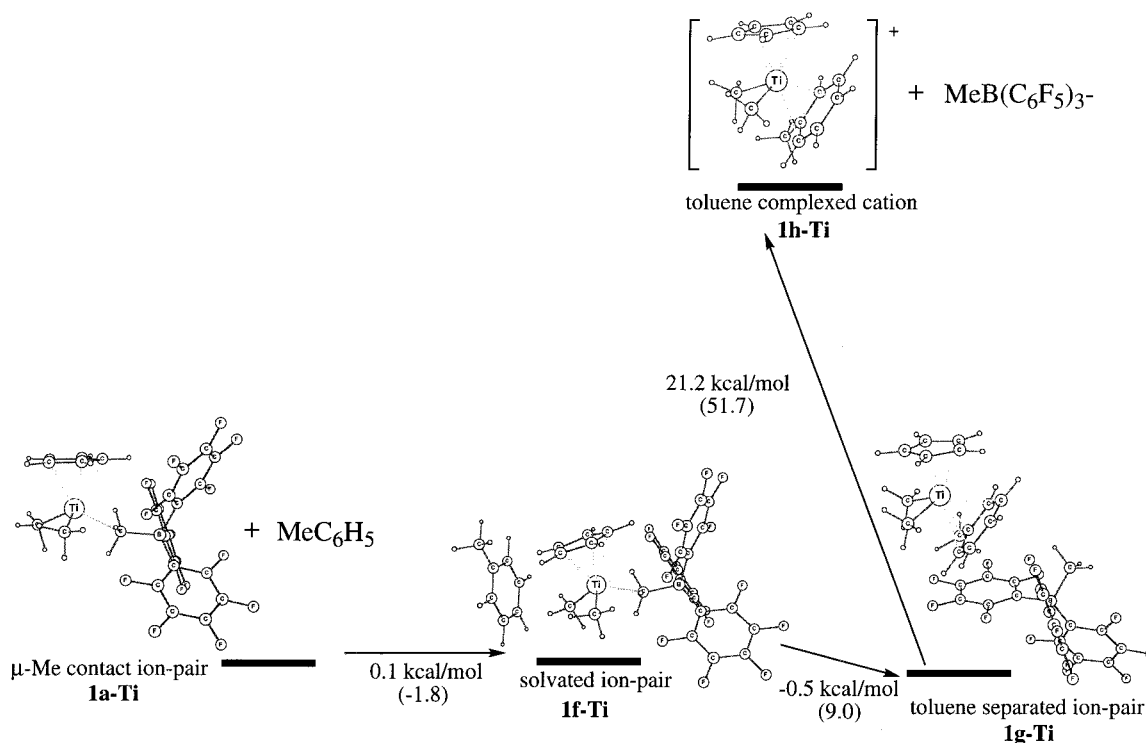


Figure 7. Toluene-complexed ions and ion pairs from the CpTiMe₃ precursor.

(**1f-Ti**) shows that the midpoint of the toluene aromatic ring is located 4.910 Å from the titanium on the opposite side of the anion and in a plane perpendicular to the Cp ring. There is also no significant change in the geometry of the contact ion pair moiety, suggesting little explicit interaction between the toluene and **1a-Ti**. Further solvation of the contact ion pair results in the formation of a solvent-separated ion pair (**1g-Ti**) where the toluene molecule is located between the cation and the anion. As can be seen from the structure shown in Figure 7, the toluene adopted an η^6 coordination to induce a geometry similar to the bis(cyclopentadienyl) structure for the cationic moiety. The anion has also turned in such a way that one of the aryl groups is pointing toward toluene. This ion pair is 7.2 kcal/mol higher in energy than the contact ion pair (**1a-Ti**) and a free molecule of toluene in the gas phase; however, correcting for solvent effects brings it down in energy to be just slightly more stable than **1a-Ti** at -0.4 kcal/mol. Dissociation of the solvent-separated ion pair led to the formation of the solvent-complexed cation (**1h-Ti**) and the anion MeB(C₆F₅)₃⁻, which are 20.8 kcal/mol less stable than the contact ion pair (**1a-Ti**), indicating that the anion still provides significant stabilization to the toluene-complexed cationic metal fragment. The relative energies of these toluene-associated species are in agreement with experimental results performed on the pentamethylcyclopentadienyl system.²² Addition of equimolar amounts of (C₅Me₅)TiMe₃ and B(C₆F₅)₃ in a solution of hexane/toluene (10:1) resulted in the formation of a μ -Me ion pair that can be detected by ¹H NMR spectroscopy. Addition of small amounts of toluene to a CD₂Cl₂ solution of this ion pair resulted in partial (~30%) conversion to the [(C₅Me₅)-TiMe₂(η^6 -MeC₆H₅)] [MeB(C₆F₅)₃] complex.

The potential energy surface of the CpZrMe₃ system (Figure 8) is similar to that of the titanium system, with the exception that the toluene-separated ion pair (**1g-Zr**) is now more stable than the contact ion pair (**1a-Zr**) by 8.0 kcal/mol. This increase in stability over the titanium system has also been observed experimentally with the pentamethylcyclopentadienyl system. Addition of equimolar amounts of (Me₅C₅)ZrMe₃ and B(C₆F₅)₃ in a solution of hexane/toluene (10:1) resulted in almost quantitative formation of a [(Me₅C₅)ZrMe₂(η^6 -MeC₆H₅)] [MeB(C₆F₅)₃] complex that was isolated as a solid as opposed to the formation of the contact ion pair in the titanium system.²² Further dissociation of this solvent-separated ion pair (**1g-Zr**) into the solvent-complexed cation (**1h-Zr**) and the anion is endothermic by 20.4 kcal/mol in solution.

The potential energy surface for the formation of complexes and ion pairs in the presence of toluene is shown in Figures 9 and 10 for the constrained-geometry systems H₂SiCp(NH)TiMe₂ and H₂SiCp(NH)ZrMe₂, respectively. The solvated ion pairs (**2f-Ti** and **2f-Zr**) with one molecule of toluene treated quantum mechanically is much more stabilized than the mono(cyclopentadienyl) system at -4.2 kcal/mol for the titanium and -5.2 kcal/mol for the zirconium. In these systems, the aromatic ring of the toluene is parallel to the Cp ring and is located below the cationic moiety of the contact ion pair. The relatively large "solvation" energy obtained for the constrained-geometry systems may be a result of substituting the *tert*-butyl group in the amido ligand with a hydrogen atom in the calculations. The absence of this bulky functional group allows for a closer approach of the toluene molecule to the positive metal center, thus increasing the solvent-solute interaction. The insertion of the toluene molecule into the contact ion pairs (**2a-Ti** and **2a-Zr**) to form the solvent-separated ion pairs (**2g-Ti** and **2g-Zr**) is endothermic

(22) Gillis, D. J.; Tudoret, M.-J.; Baird, M. C. *J. Am. Chem. Soc.* **1993**, *115*, 2543.

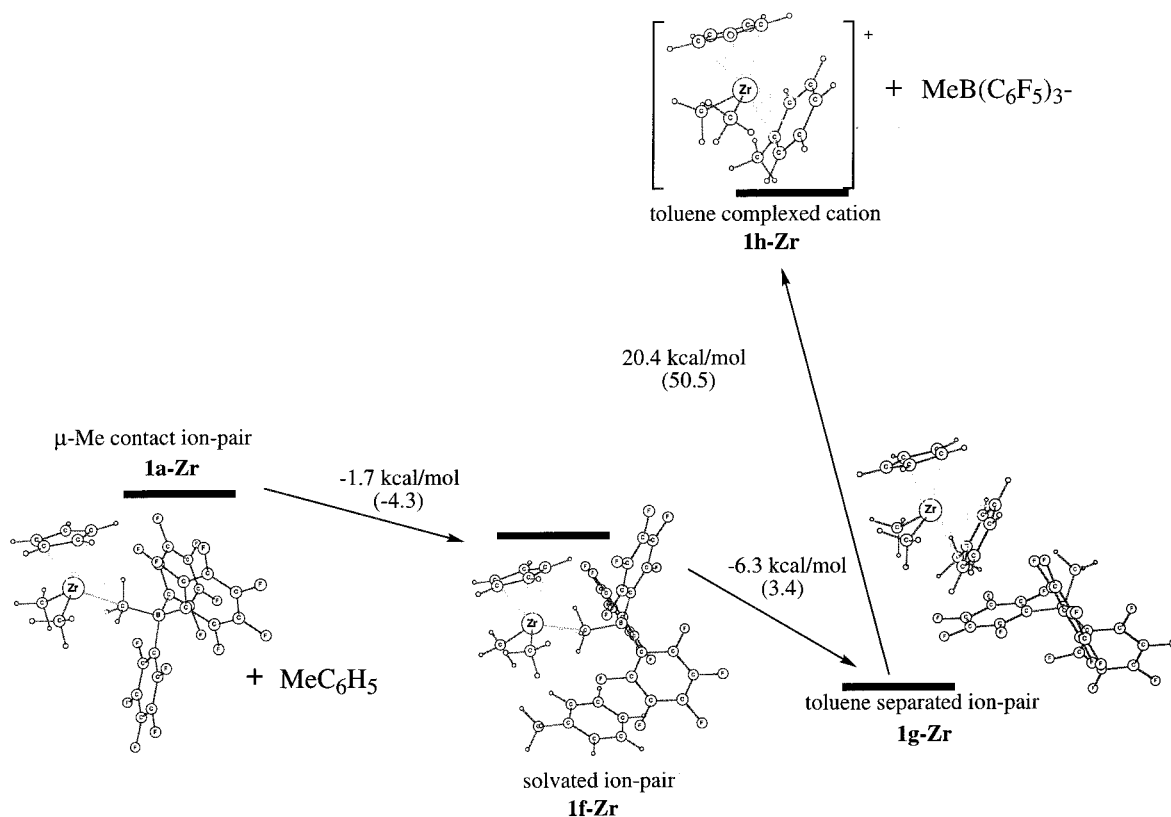


Figure 8. Toluene-complexed ions and ion pairs from the CpZrMe_3 precursor.

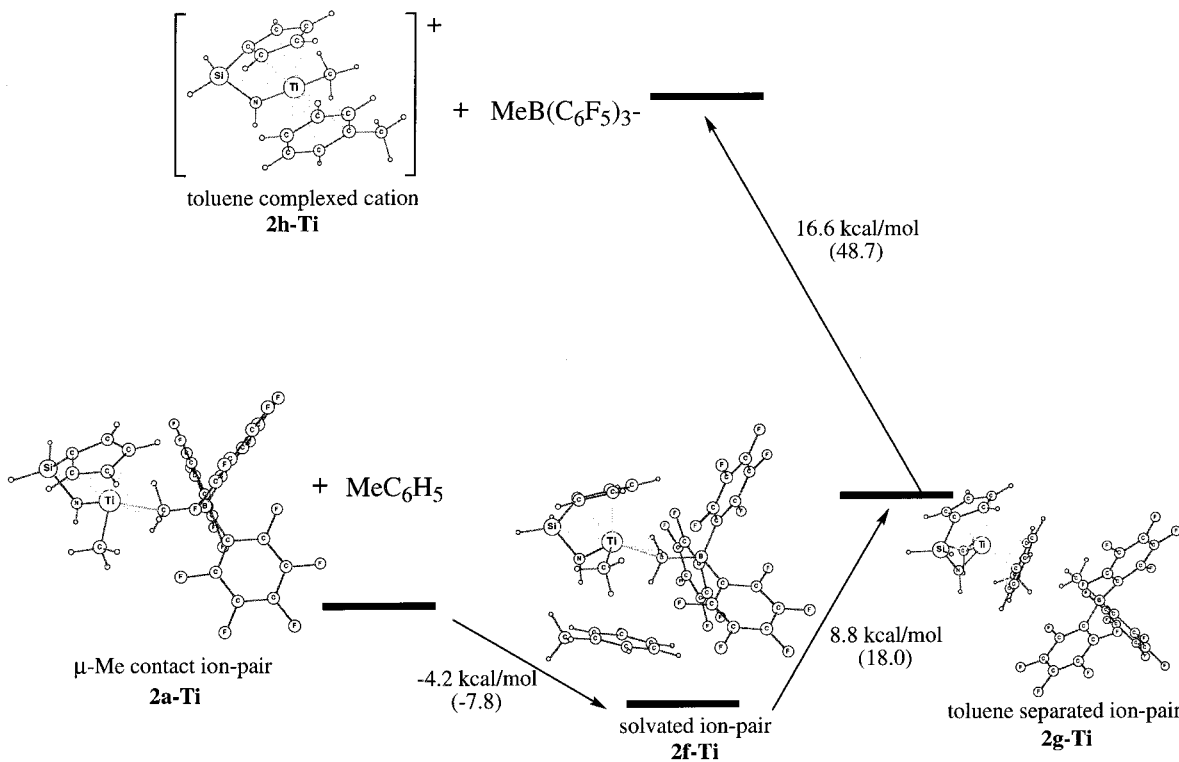


Figure 9. Toluene-complexed ions and ion pairs from the $\text{H}_2\text{SiCp(NH)TiMe}_2$ precursor.

by 8.8 kcal/mol for the titanium, while it is thermally neutral for the zirconium system. This is consistent with the much stronger toluene binding energy observed for the zirconium in the mono(cyclopentadienyl) system. The dissociation into the toluene-complexed cation (**2h-Ti** and **2h-Zr**) and anion requires 16.5 and 16.7 kcal/mol for the titanium and zirconium, respectively.

The potential energy surface for the formation of toluene-complexed ion pairs is shown in Figure 11 for the titanium bis(cyclopentadienyl) system. The potential energy surface for the zirconium analogue shows similar features and is therefore not shown. The solvated ion pairs (**3f-Ti** and **3f-Zr**) with one molecule of toluene attached are now on the order of $2.5\text{--}3.0 \text{ kcal/mol}$ more

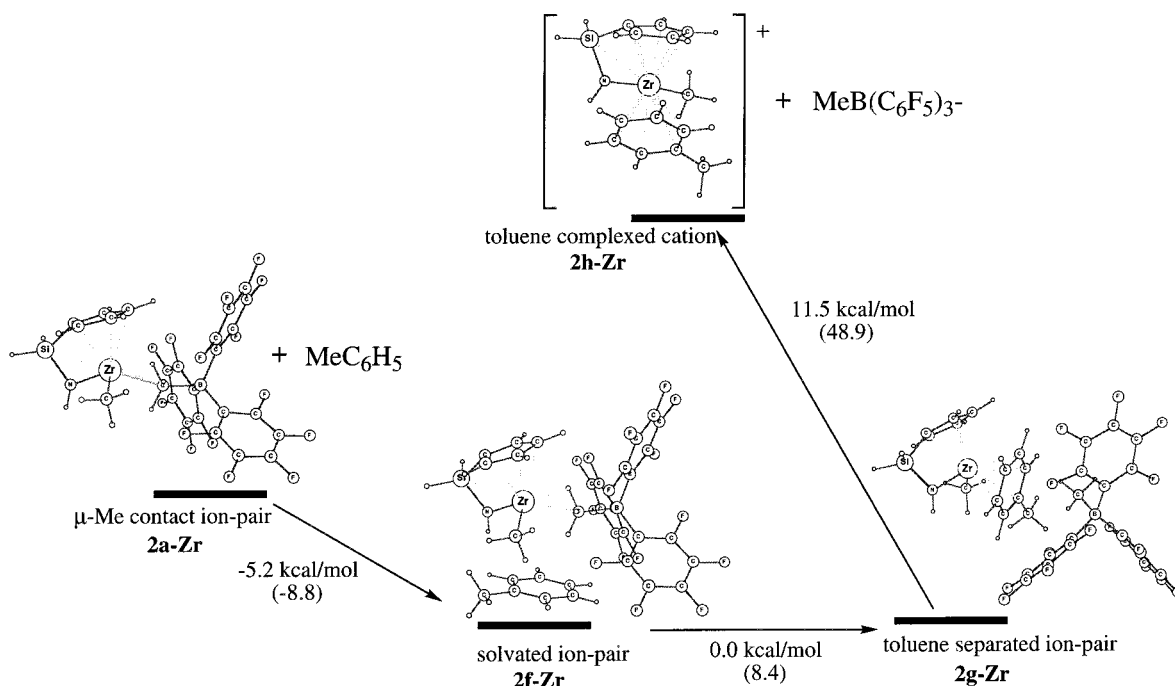


Figure 10. Toluene-complexed ions and ion pairs from the $\text{H}_2\text{SiCp}(\text{NH})\text{ZrMe}_2$ precursor.

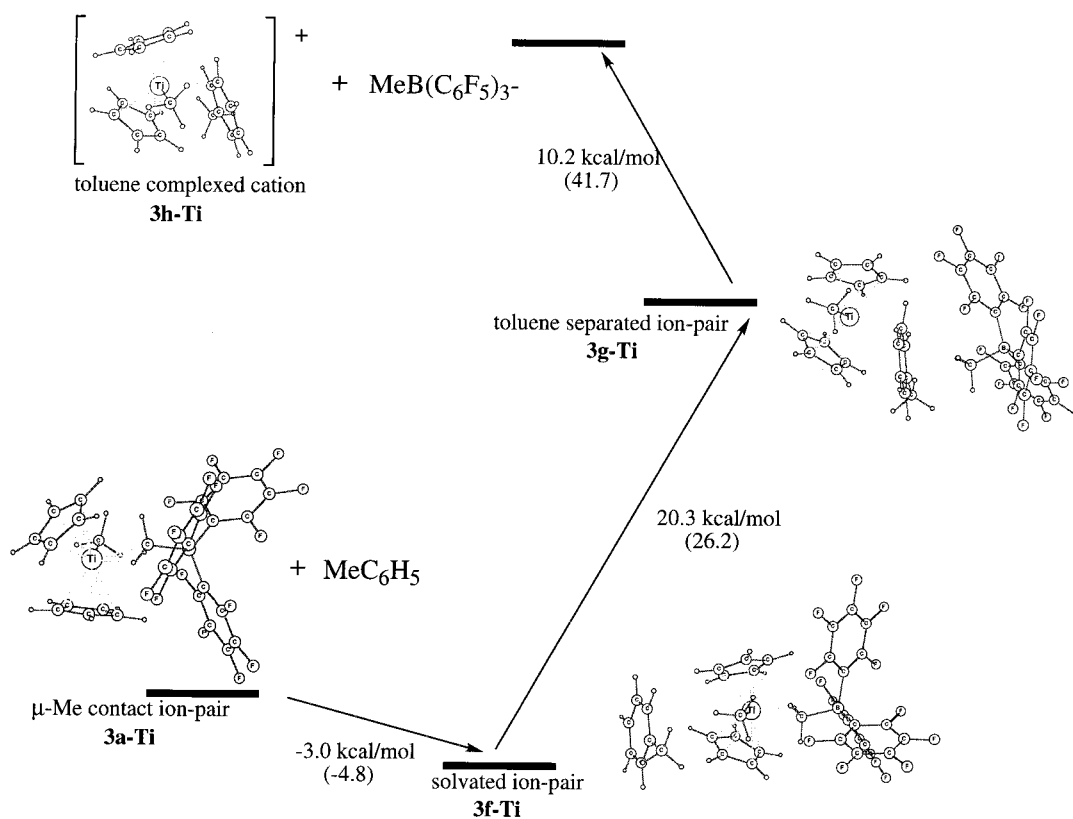
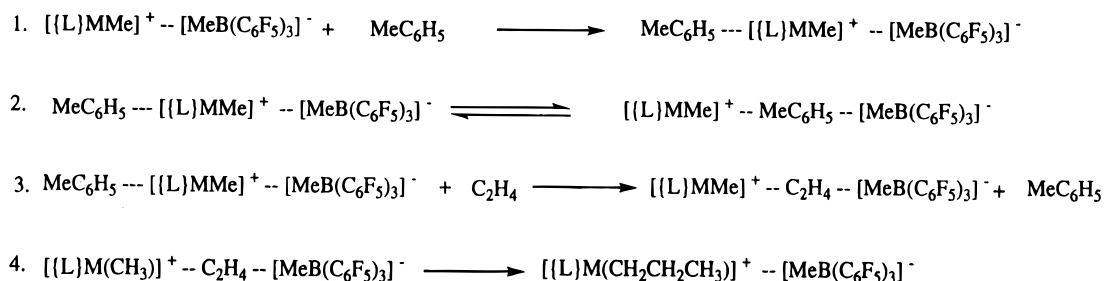


Figure 11. Toluene-complexed ions and ion pairs from the Cp_2TiMe_2 precursor.

stable than the contact ion pairs (**3a-Ti** and **3b-Zr**), suggesting that the explicit interaction between the contact ion pair with the solvent toluene is larger than that for the mono(cyclopentadienyl) catalysts but slightly smaller than that for the constrained-geometry catalysts. The most marked contrast between these systems and the two discussed previously is the difference in stability of toluene-separated ion pairs (**3g-Ti** and **3g-Zr**), which now lies 20.3 and 17.1 kcal/mol above the

solvated ion pairs (**3f-Ti** and **3f-Zr**). The main reason for the relative instability of these species with regard to their mono(cyclopentadienyl) and constrained-geometry analogues can be attributed to steric factors. The second cyclopentadienyl ligand takes up more room around the metal center than a methyl ligand or an amido ligand. The steric bulk of the second Cp ring prevents the approach of the toluene, resulting in an η^2 rather than an η^6 coordination mode. The combina-

Scheme 2. Proposed Mechanism of Activation for the Mono(cyclopentadienyl) and Constrained-Geometry Precursors

tion of excess steric repulsion and the decreased electronic stabilization provided by the toluene makes the solvent-separated ion pairs (**3g-Ti** and **3g-Zr**) unfavorable intermediates. Further dissociation into the completely separated toluene-complexed cations (**3h-Ti** and **3h-Zr**) and anions causes a gain of only 10.2 kcal/mol for the titanium and 11.0 kcal/mol for the zirconium, suggesting that the anion plays a less stabilizing role than in the mono(cyclopentadienyl) system.

(iii) Implications for the Initial Stages of Ethylene Polymerization. The above data suggest that changes in the ancillary ligands of the catalyst precursor can have a strong influence on the possible mechanism for ethylene complexation. Two distinctively different pathways emerge from the study of the three catalyst systems examined. The first pathway is associated with the mono(cyclopentadienyl) and the constrained-geometry catalyst systems. These precursors were first investigated with the hypothesis that they would achieve higher catalytic activities than their bis(cyclopentadienyl) counterparts. The reasoning behind this was that the activated catalysts would be more electrophilic and less sterically hindered, allowing for more facile complexation of the olefin.²³ While this may be true for the "bare" cations such as **1d** and **2d**, our calculations suggest that the initial complexation of the olefin to the contact ion pairs (**1a** and **2a**) is endothermic. Dissociation of the contact ion pairs (**1a** and **2a**) to produce the coordinatively unsaturated cations (**1d** and **2d**) was found to be highly endothermic, and therefore, it is unlikely that these species will be present with an appreciable concentration in the reaction mixture. In fact, the energetics show that the species with the cation and anion at infinite separation are at least 14 kcal/mol higher in energy than their analogues with the anion still in the vicinity, stressing the importance of the counterion or cocatalyst.

A proposed mechanism for the initial stages of ethylene polymerization based on our calculations is depicted in Scheme 2. With the neutral precursors as starting materials, the most likely species that will form is the contact ion pair. In toluene, this contact ion pair can subsequently rearrange to the solvated ion pair (step 1 of Scheme 2) followed by the solvent-separated ion pair where one molecule of toluene is bound to the metal cationic moiety (step 2 of Scheme 2). Both experimental evidence (as discussed in the above section) and the small calculated energy difference between the two species support the notion that the contact ion

pair and the toluene-separated ion pair are in equilibrium. There are significant amounts of both species present for the titanium systems, while the equilibrium lies far to the right (in favor of the toluene-separated ion pair) in the zirconium systems. Nevertheless, the formation of the toluene-separated ion pair should be reversible. Once at the toluene-separated ion pair, the possible reaction pathways are going back to the contact ion pair or proceeding to the solvent-separated ions. The pathway back to the contact ion pair is the energetically more favorable process. Therefore, there should be a nonzero (albeit small) concentration of the contact ion pair in solution at all times to facilitate ethylene complexation (step 3 of Scheme 2). Previous studies without the counterion have indicated that step 4 of Scheme 2, where the complexed olefin inserts into the growing polymer chain, proceeds with little or no barrier.²⁴

The second mechanism is associated with the bis(cyclopentadienyl) systems. The steps are related to the mechanism proposed for the mono(cyclopentadienyl) and constrained-geometry systems with the exception that the second step is thermodynamically unfavorable, with the equilibrium lying far to the left. The steric bulk of the two cyclopentadienyl ligands prevents the coordination of the metal center with the toluene, making ethylene complexation a more favorable pathway. Activation of the catalyst precursor leads to the formation of the contact ion pair, and this will proceed directly to the olefin-separated ion pair, as the steric hindrance provided by the two Cp ligands is less felt by the olefin because of its small size. Therefore, the bis(cyclopentadienyl) systems should be the best catalysts of the three systems investigated, consistent with experimental observations.²⁵ This proposed mechanism for the bis(cyclopentadienyl) systems contains features similar to those for the titanocene/MAO and zirconocene/MAO systems studied by Fusco et al.^{6b-d} In their calculations, these authors found that the reaction of the metallocene with the cocatalyst to produce a 1:1 contact ion pair is an exothermic process. Subsequent olefin complexation with this contact ion pair is an endothermic process, due to the displacement of the counterion from the metal center, although this is still the least unfavorable pathway to polymerization. The present calculations and the work of Fusco indicate that olefin-separated ion pairs are key intermediates for olefin polymerization

(24) Woo, T. K.; Fan, L.; Ziegler, T. *Organometallics* **1994**, *13*, 2252.

(25) Yang, X.; Stern, C. L.; Marks, T. J. *J. Am. Chem. Soc.* **1994**, *116*, 10015.

(26) Brintzinger, H. H.; Fischer, D.; Mülhaupt, R.; Rieger, B.; Waymouth, R. M. *Angew. Chem., Int. Ed. Engl.* **1995**, *34*, 1143.

(23) Sarsfield, M. J.; Ewart, S. W.; Tremblay, T. L.; Roszak, A. W.; Baird, M. C. *J. Chem. Soc., Dalton Trans.* **1997**, 3097.

and confirms the hypothesis put forth by Brintzinger of the importance of the formation of olefin-separated ion pairs in the polymerization mechanism.²⁶

The above proposed mechanisms are specific to polymerization that is carried out with toluene as the solvent. Different solvents have different coordinating abilities and, therefore, will influence the relative stability of the solvent-separated ion pairs. The polarity of the solvent will also influence the relative stability of the complexed ion pairs relative to the separated ions. The results of this study indicate that polymerization would be more facile in the presence of less coordinating solvents. A solvent with a higher dielectric constant would encourage charge separation, favoring the formation of solvent-separated ions rather than ion pairs. This would also help facilitate polymerization because the cationic metal center is more accessible to the incoming olefin. An earlier study by Eisch et al.²⁷ on the $\text{Cp}_2\text{TiCl}_2/\text{AlCl}_3$ and $\text{Cp}_2\text{Ti}(\text{CH}_2\text{SiMe}_3)/\text{AlCl}_3$ systems has found that the dominant type of ion pair present is dependent on the experimental conditions such as polarity and donor character of the solvent, concentration of the catalyst, and temperature. Their results from polymerization studies suggested that the noncoordinated cation is the most reactive, followed by the contact ion pair, and finally the arene-separated ion pair if the reaction was performed in arene solvents. Another limitation of these mechanisms is that they only address the complexation of the first olefin molecule. This was found to be an endothermic process because the energy required to break the methyl bridge in the contact ion pair is larger than the energy gained by olefin coordination. In polymerization reactions where there is a high concentration of the olefin, complexation of subsequent olefin molecules may occur before the contact ion pair has a chance to reestablish itself after the first insertion. If this is the case, such complexation will be exothermic and the polymerization would proceed in much the same way as indicated by previous studies without the counterion. The need to break the contact ion pair for the first olefin complexation may be one of the factors responsible for the induction period before continuous uptake of olefin that had been observed for some zwitterionic systems.²⁸

(27) Eisch, J. J.; Pombrik, S. I.; Zheng, G.-X. *Organometallics* **1993**, *12*, 3856.

(28) Svejda, S. A.; Brookhart, M. *Organometallics* **1999**, *18*, 65.

IV. Conclusions

A density functional study was conducted on the methide abstraction by $\text{B}(\text{C}_6\text{F}_5)_3$ from the mono(cyclopentadienyl), constrained-geometry, and bis(cyclopentadienyl) catalyst precursors to form a contact ion pair. The calculations showed that the electron-donating ability of the ligands is the most predominant factor in determining the enthalpy for the activation reaction. The higher the electron-donating ability of the ligands attached to the metal center, the more negative the enthalpy of abstraction becomes. The steric bulk of the ligands plays a small, but still significant, role in determining the magnitude of the enthalpy change.

The reactions of the contact ion pair with ethylene and with the solvent (toluene) were also investigated. The insertion of the ethylene into this contact ion pair was found to be an endothermic process for all of the catalyst systems studied. The insertion of the toluene between the contact ion pair is exothermic for both of the mono(cyclopentadienyl) systems and the zirconium constrained-geometry catalyst but endothermic for the titanium constrained-geometry system and both of the bis(cyclopentadienyl) catalysts. The bis(cyclopentadienyl) catalysts are predicted to have the highest activity, on the basis of the theoretical results of the present study. The steric bulk of the Cp rings prevents the approach of the toluene, making complexation with the ethylene more favorable. In general, catalysts with large ligands should be more effective in polymerizing small olefins in bulky solvents. For catalysts with less steric bulk, such as the mono(cyclopentadienyl) and constrained-geometry catalysts, coordination with the toluene is more favorable than with the ethylene. These catalysts would show better performance in less coordinating solvents.

Acknowledgment. This investigation was supported by the Natural Science and Engineering Research Council of Canada (NSERC) and by Novacor Research and Technology (NRTC) of Calgary, Alberta, Canada.

Supporting Information Available: Tables of gas-phase energies, solvation energies, and Cartesian coordinates of DFT-optimized structures **1(a-h)(Ti-Zr)**, **2(a-h)(Ti-Zr)**, and **3(a-h)(Ti-Zr)**. This material is available free of charge via the Internet at <http://pubs.acs.org>.

OM9903285